

CHAPTER 104

BEHAVIOR OF A SLENDER BODY IN SHALLOW-WATER WAVES

by

Hsiang Wang*

and

Li-San Hwang**

Abstract

The unsteady-state response of a slender body in nonlinear shallow-water wave environment was studied. Numerical scheme has been developed which permits rapid calculation of the following, which describe the motion of an arbitrarily shaped body in three degrees of freedom anywhere within such an environment:

- a Unsteady-state response
- b Centroid locus
- c Forces and moments

Sample calculations are given for a typical submersible. Results are expressed in generalized parameters, defining the circumstances wherein various displacements, velocities, accelerations, etc., would occur.

Introduction

The primary objective of the present work was to study the unsteady state response of a slender body in nonlinear shallow-water wave environment. Consideration was restricted to the wave-induced motions of a rigid body confined to one plane, hence, involving only three degrees of freedom--either surge, pitch, and heave, or sway, heave, and roll. This would correspond to the case when the wave is long-crested and is incidental along the body in the former case and is incidental to the broad side in the latter case.

The hydrodynamic forces under consideration consist of four parts: pressure and inertial forces that can be derived from velocity potential, drag force that is proportional to the square of the relative velocity, restoring force due to the relative position and orientation of the body in the fluid, and thrust and uprighting moment due to the body.

* University of Delaware, Newark, Delaware 19711

** Tetra Tech, Inc., Pasadena, California 91107

The seaway which enters as the input to the system, is derived from the following wave theories

- a Cnoidal wave theory of Keulegan and Patterson for high, long, near-breaking and breaking waves
- b Airy linear theory for short period waves
- c McCowan solitary wave theory of matching period for very long waves

These theories are chosen on the basis that they provide the best approximation to internal wave characteristics as obtained experimentally

A numerical scheme has been developed which permits rapid calculation of the following, which describe the motion of an arbitrarily shaped body in three degrees of freedom anywhere within such an environment

- a Unsteady-state response
- b Centroid locus
- c Forces and moments

Results are expressed in generalized parameters, defining the circumstance wherein various displacements, velocities, accelerations, etc , would occur

The Equations of Motion of a Submerged Body

Consideration was restricted to the wave-induced motions of a rigid submerged body confined to one plane, hence involving only three degrees of freedom--either surge, pitch, and heave or sway, heave, and roll, as defined on Figure 1 This would correspond to the case when the wave is long-crested and is incident to along the body in the former case and incident to the broad side in the latter Although, in principle, these two cases are the same hydrodynamically, they differ somewhat in the method of obtaining an engineering solution

Two sets of coordinate systems were employed in analyzing the responses of a submerged body, they are

- a Fixed coordinate system used to describe the sea conditions and the position of the body, the origin is arbitrary and was chosen here at the sea bottom with the x-axis parallel to the longitudinal axis of the body, the y-axis pointing upward vertically, and the z-axis in the transverse direction
- b Body coordinate system used to describe the oscillations of the body The body had three principal axes, hence six degrees of freedom, corresponding to a translation and a rotation for each axis Symbol definitions are shown in Figure 1 The body axes have their origin at the center of gravity of the body and are coincident with the intersections of the principal planes of inertia

The problem of body response in a wave environment is treated in four steps

- a Derivation of flow environment
- b Derivation of hydrodynamic excitation
- c Derivation of body response and tracing of locus of body motion
- d Derivation of forces exerted on the body

Incident Wave Parallel to the Longitudinal Axis

For motions confined to the xy-plane, it is assumed that motion is described by three functions of time $X(t)$, $Y(t)$, and $\theta(t)$, which are such that the location of the center of gravity of the body is (X, Y) at time t , and the angle of inclination of the body is θ (Figure 1). Then the equations of motion of the body are

$$\left. \begin{aligned} M\ddot{X} &= F_x \\ MY &= F_y \\ I_\theta \ddot{\theta} &= F_\theta \end{aligned} \right\} (1)$$

where M is the natural mass, I_θ is the pitching moment of inertia, and F_x , F_y , and F_θ are the total hydrodynamic forces and moments on the body. The main problem is, of course, the estimation of these hydrodynamic forces.

It is convenient to separate the hydrodynamic forces into four parts: pressure and acceleration forces that can be derived from velocity potential, velocity force that has to be estimated using empirical drag coefficient, restoring force due to the relative position and orientation of the body in the fluid, and thrust or uprighting moment provided by the body.

For a body which is slender (i.e., has small cross-section relative to its length and to a typical wave length), the pressure forces, or Froude-Krylov forces (Korvin-Kroukovsky, 1961), are relatively easy to estimate. Suppose the given incident pressure field is $p(x, y, t)$ and the local horizontal and vertical pressure gradients at a station ξ of the body are calculated

$$P(\xi, t) = \frac{\partial p}{\partial x}(\lambda + \xi \cos \theta, Y + \xi \sin \theta, t) \quad (2)$$

$$Q(\xi, t) = \frac{\partial p}{\partial y}(X + \xi \cos \theta, Y + \xi \sin \theta, t) \quad (3)$$

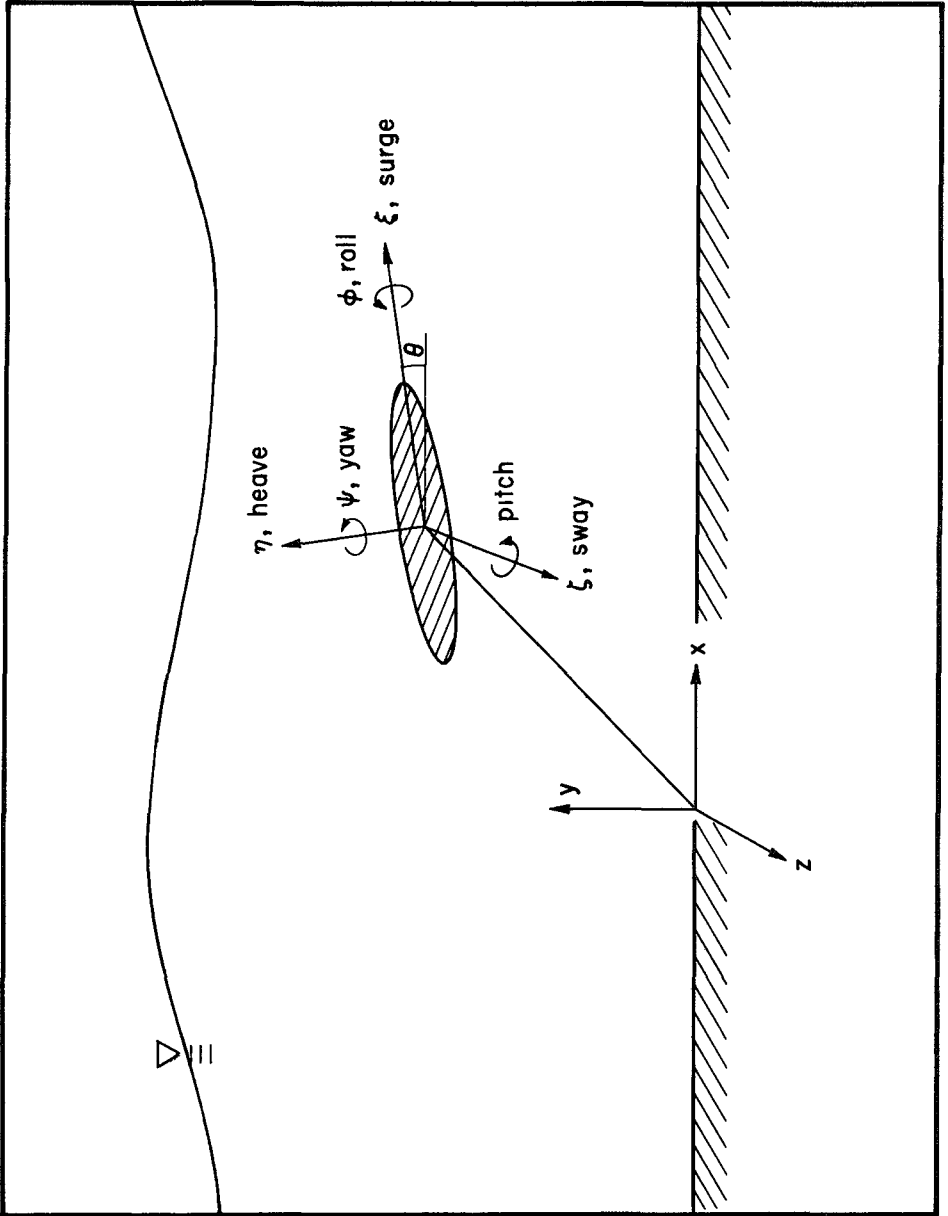


Figure 1 Coordinate system

then the pressure forces are easily seen to be

$$F_x^{FK} = - \int_{\ell} P(\xi, t) S(\xi) d\xi \quad (4)$$

$$F_y^{FK} = - \int_{\ell} Q(\zeta, t) S(\xi) d\xi \quad (5)$$

and the pitching moment is

$$F_{\theta}^{FK} = -\cos\theta \int_{\ell} \xi Q(\zeta, t) S(\xi) d\xi + \sin\theta \int_{\ell} \xi P(\xi, t) S(\xi) d\xi \quad (6)$$

Here $S(\xi)$ is the area of the cross-section of the body at station ξ , and the integrations extend over the length of the body. The acceleration forces include that due to the motion of the body and that due to the diffraction of the wave field by the body. If the body is slender, its effect on the fluid is sensible only when there is a relative motion across its axis. Thus, the longitudinal added mass of a spheroid with a thickness ratio 1 in 10 is only 2 percent of the displaced mass (Lamb, 1932), whereas the lateral added mass is nearly equal to the displaced mass. Hence, "strip" methods may be used to obtain the added inertia effects by considering only the cross flow at each station ξ . The fluid in the neighborhood of station ξ has an acceleration

$$\frac{1}{\rho} P(\xi, t) \sin\theta - \frac{1}{\rho} Q(\xi, t) \cos\theta$$

normal to the body axis, whereas the body itself has acceleration

$$-\ddot{X} \sin\theta + \ddot{Y} \cos\theta + \xi \ddot{\theta}$$

Hence, there is a relative acceleration of the section at ξ of

$$a(\xi) = -\left(\ddot{X} + \frac{1}{\rho} P\right) \sin\theta + \left(\ddot{Y} + \frac{1}{\rho} Q\right) \cos\theta + \xi \ddot{\theta} \quad (7)$$

The cross flow, or slender-body hypothesis, now asserts that the hydrodynamic effect of this relative motion is an opposing force $\mu(\xi)a(\xi)d\xi$ on a section of thickness $d\xi$, where $\mu(\xi)$ is the added mass of the section, calculated as if the flow were two dimensional, irrotational, and infinite in extent. Resolving horizontally and vertically and taking moments, we have inertia terms

$$F_x^A = - \int_l \mu(\xi)a(\xi)d\xi \sin\theta \quad (8)$$

$$F_y^A = \int_l \mu(\xi)a(\xi)d\xi \cos\theta \quad (9)$$

$$M_0^A = \int_l \xi \mu(\xi)a(\xi)d\xi \quad (10)$$

The force generated through the relative velocity between the body and the fluid flow is associated with the momentum defect of the fluid due to the body. This force is generally expressed in the form

$$F_D = \rho \frac{C_D}{2} A |V|V \quad (11)$$

where

C_D = drag coefficient

A = frontal area (normal to flow)

V = relative flow velocity

The drag coefficient is a function of Reynolds number and differs for different body geometry. The velocity force in the cross-flow direction and longitudinal-flow direction can be written separately as

$$\begin{aligned} F_{D\eta} &= \rho \frac{1}{2} \int_l C_D |V_{R\eta}| V_{R\eta} dA \\ &= \rho \frac{C_{DC}}{2} \int_l |V_{R\eta}| V_{R\eta} dA \end{aligned} \quad (12)$$

and

$$\begin{aligned}
 F_{D\xi} &= \rho \frac{1}{2} \int_B C_D |V_{R\xi}| V_{R\xi} dA \\
 &= \rho \frac{C_{DL}}{2} \int_B |V_{R\xi}| V_{R\xi} dA
 \end{aligned} \tag{13}$$

where

- $F_{D\eta}$ = drag force in the cross-flow direction
- $F_{D\xi}$ = drag force in the longitudinal-flow direction
- F_{DC} = average drag coefficient in the cross-flow direction
- F_{DL} = average drag coefficient in the longitudinal-flow direction

and the integral limits l and B denote that the integrations are performed along the longitudinal axis and along the vertical axis of the body

The relative velocities in the cross-flow direction $V_{R\eta}$ and in the longitudinal direction $V_{R\xi}$ are, respectively,

$$V_{R\eta} = -U_R \sin\theta + V_R \cos\theta + \xi \dot{\theta} \tag{14}$$

$$V_{R\xi} = U_R \cos\theta + V_R \sin\theta \tag{15}$$

with U_R and V_R defined as

$$U_R = X - u \tag{16}$$

$$V_R = Y - v \tag{17}$$

where X and Y are the velocity components of the body in the x - and y -directions and u and v are the velocity components of the fluid in the x - and y -directions

Again, like inertia terms, resolving horizontally and vertically and taking moments to obtain the drag forces

$$F_x^D = -F_{Dz} \cos \theta + \Gamma_{D\eta} \sin \theta \quad (18)$$

$$F_y^D = -F_{Dz} \sin \theta - \Gamma_{D\eta} \cos \theta \quad (19)$$

$$\Gamma_{\theta}^D = -\rho \frac{C_{DC}}{2} \int_{\ell} \xi |V_{R\eta}| V_{R\eta} dA \quad (20)$$

The restoring forces are simply

$$F_x^R = 0 \quad (21)$$

$$\begin{aligned} F_y^R &= -w_s && \text{for partial submergence} \\ &= 0 && \text{for full submergence} \end{aligned} \quad (22)$$

where w_s is the partial weight of the body that is surfaced

The restoring moments are

$$F_{\theta}^R = -\rho g \Psi_s \bar{ee} \sin \theta - \cos \theta \int_{\ell_1} \rho_s g \xi dV \quad (23)$$

for partial submergence and

$$F_{\theta}^R = -\rho g \Psi_s \bar{ee} \sin \theta$$

for full submergence

where

- Ψ_s = volume of displaced water
- ee = metacentric height of body
- ρ = density of sea water
- ρ_s = density of body
- ℓ_1 = body length above free surface

Finally, the thrust and righting moments produced by the body when resolved into x-, y-, and θ -directions, are

$$F_x^T = T_t \cos \theta \tag{21}$$

$$F_y^T = T_t \sin \theta \tag{25}$$

$$F_\theta^T = -M_r \theta \tag{26}$$

where T_t is the thrust, and $M_r \theta$ is the righting moment, which is assumed to be proportional to the pitch angle

Thus, we have completed the disposition of the total forces acting on the body, and the equations of motion become

$$\left. \begin{aligned} MX &= F_x^{FK} + F_x^A + F_x^D + F_x^T \\ MY &= F_y^{FK} + F_y^A + F_y^D + F_y^R + F_y^T \\ I_\theta \dot{\theta} &= F_\theta^{FK} + F_\theta^A + F_\theta^D + F_\theta^R + F_\theta^T \end{aligned} \right\} \tag{27}$$

When expressed explicitly, the equations of motion are

$$\left. \begin{aligned} M\ddot{X} &= - \int_l P(\xi, t) S(\xi) d\xi - \int_l u(\xi) a(\xi) d\xi \sin \theta - \rho \frac{C_{DL}}{2} \int_B |V_{R\xi}| |V_{R\xi}| dA \cos \theta \\ &\quad + \rho \frac{C_{DC}}{2} \int_l |V_{R\eta}| |V_{R\eta}| dA \sin \theta + T_t \cos \theta \\ MY &= - \int_l Q(\xi, t) S(\xi) d\xi + \int_l u(\xi) \eta(\xi) d\xi \cos \theta - \rho \frac{C_{DL}}{2} \int_B |V_{R\xi}| |V_{R\xi}| dA \cos \theta \\ &\quad - \rho \frac{C_{DC}}{2} \int_l |V_{R\eta}| |V_{R\eta}| dA \cos \theta + T_t \sin \theta + F_y^R \\ I_\theta \ddot{\theta} &= - \cos \theta \int_l \xi Q(\xi, t) S(\xi) d\xi + \sin \theta \int_l \xi P(\xi, t) S(\xi) d\xi + \int_l \xi u(\xi) a(\xi) d\xi \\ &\quad - \rho \frac{C_{DC}}{2} \int_l \xi |V_{R\eta}| |V_{R\eta}| dA - M_r \theta + F_\theta^R \end{aligned} \right\} \tag{28}$$

where F_y^R and F_θ^R are defined in Eqs 22 and 23, respectively. Once the flow field has been described, these three simultaneous equations can be solved using a high-speed computer.

The surging force, heaving force, and pitching moment are evaluated, respectively, according to the following equations

$$F_\xi = M(X\cos\theta + Y\sin\theta) - I_\theta(\dot{\theta})^2 \quad (29)$$

$$F_\eta = M(X\sin\theta + Y\cos\theta) - I_\theta\ddot{\theta} \quad (30)$$

$$M_T = I_\theta\dot{\theta} \quad (31)$$

where

F_ξ = surging force

F_η = heaving force

M_T = pitching moment

Incident Wave Perpendicular to the Longitudinal Axis

The equations of motion are similar to the previous case, except the evaluation of some forces were different. In the determination of the mass coefficients, the main body was treated as a cylindrical body of variable diameter. The drag term was calculated in a much similar way as the acceleration term, with due consideration in choosing drag coefficients for different parts.

The calculation of pressure force, and restoring force, remains the same as in the case of parallel waves. The complete calculations of motion for sway, heave, and roll, when expressed in force components, are, respectively,

$$\left. \begin{aligned} MZ &= \Gamma_z^K + \Gamma_z^A + \Gamma_z^D \\ M\dot{Y} &= \Gamma_y^K + F_y^A + \Gamma_y^D + F_y^T + \Gamma_y^R \\ I_\varphi\dot{\varphi} &= \Gamma_\varphi^K + \Gamma_\varphi^A + F_\varphi^D + \Gamma_\varphi^T + \Gamma_\varphi^R \end{aligned} \right\} (32)$$

Wave Environment and Flow Field

Three wave theories were used for evaluating excitation forces They are

- a Cnoidal wave theory of Keulegan and Patterson for high, long, near-breaking, and breaking waves
- b Airy linear theory for short period waves
- c McCowan solitary wave theory for very long waves

The cnoidal wave has wave profile (Wiegel, 1964)

$$y_s = y_t + Hcn^2 \left[2K(k) \left(\frac{x}{L} - \frac{t}{T} \right) k \right] \quad (33)$$

with wave period to the first order

$$T = \frac{4d}{\sqrt{3gH}} \left\{ \frac{kK(k)}{\sqrt{1 + \frac{H}{d} \left[-1 + \frac{1}{k^2} \left(2 - 3 \frac{E(k)}{K(k)} \right) \right]}} \right\} \quad (34)$$

The corresponding wave length is

$$L = \sqrt{\frac{16d^3}{3H}} kK(k) \quad (35)$$

where

y_s = water surface elevation measured from sea bottom

H = wave height

cn = one of the Jacobian elliptic functions

k = a real number varied from 0 to 1

$K(k)$ = elliptic integral of first kind

$E(k)$ = elliptic integral of second kind

$$y_t = H \left(\frac{d}{H} - 1 + \frac{16d^3}{3L^2H} \right) \left\{ k(k) [K(k) \quad E(k)] \right\}$$

In Eq 34, when T is plotted as a function of k for fixed d and H , it takes a form shown in Fig 2. Thus, if one starts at point A on the curve for increasing value of T , the corresponding k can increase or decrease depending upon which branch one follows. The left branch should be discarded because it corresponds to increasing values of T with decreasing values of L , which is physically meaningless. For waves of periods shorter than T_m , the Airy theory is to be applied. By differentiating Eq 34 with respect to k and equating the result to zero,

$$\frac{d}{dH} = 1 - \frac{1}{2k} \left[4 - 9 \frac{E(k)}{K(k)} + (1 - k^2) \frac{K(k)}{E(k)} \right] \quad (36)$$

for $T\sqrt{g/d} = \text{minimum}$

Thus, the value of $(T\sqrt{g/d})_{\min}$ versus d/H so obtained defines the matching line between the cnoidal wave and linear wave. It is also evident from Fig 5 that, when the elliptic parameter approaches unity, the period approaches infinity rapidly. For instance, when the k values are changed from 1 to 0.9999, the period $4K(k)$ is decreased from infinity to about 7π . In the numerical calculation, the wave period (or length) is specified, and the value of k is found by Eq 34 through iteration. For very long waves, the value of k is very nearly equal to 1, and it becomes impractical to obtain numerically the value of k through iteration. In this case, the solitary wave, which is the limiting case of the cnoidal wave, can be treated as having a finite period for many practical purposes. The upper limit of elliptic parameter has been chosen as equal to 0.9999 in the present study. Figure 3 shows the regions where the different wave theories apply.

Method of Computation

Numerical Analysis

The differential equations to be solved are a set of three simultaneous, nonlinear second-order equations. The fourth-order formula of Runge-Kutta (Hildebrand, 1956) is used to perform the numerical evaluation. This method, which extends forward the solution of differential equations from known conditions by an increment of the independent variable without using information outside this increment, has been applied extensively in solving initial value problems. In essence, the fourth-order formula evaluates the slope of the wave at the initial point, the 1/4 point, the 1/2 point, and the 3/4 point of the interval of increment. The numerical solution is then obtained in agreement with the Taylor series solution through terms of the fourth order of the interval h . The local truncated error is then of the order of h^5 , where h is the size of the increment. In the present case, the independent variable is the nondimensional time, which is equal to t/T , where t is real time, and T is the wave period.

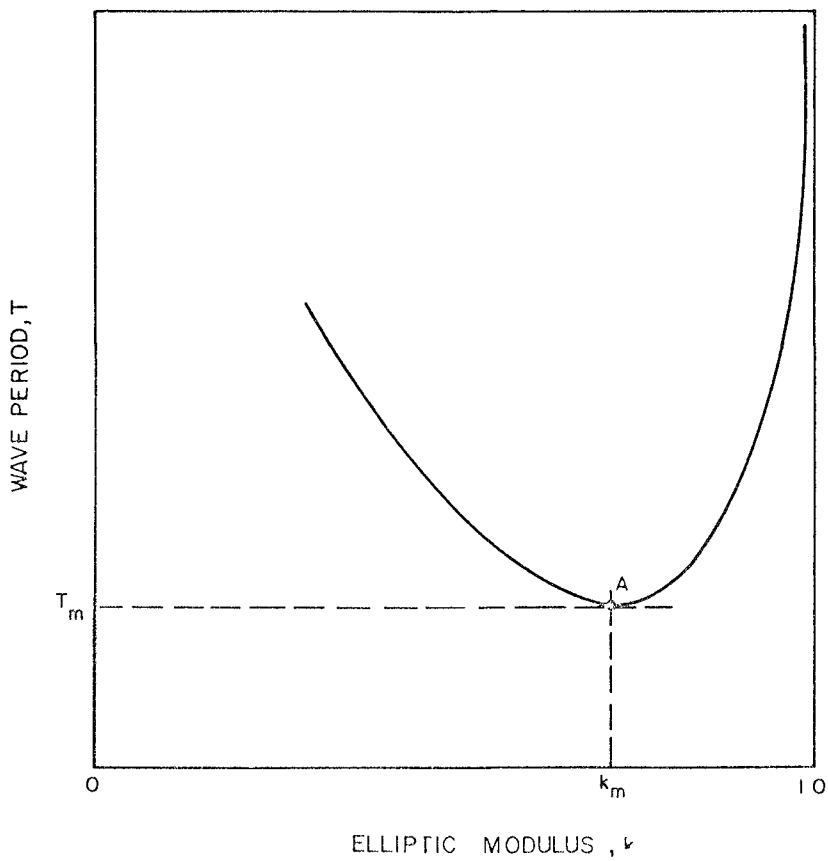


Figure 2 Wave period versus elliptic modulus for cnoidal wave

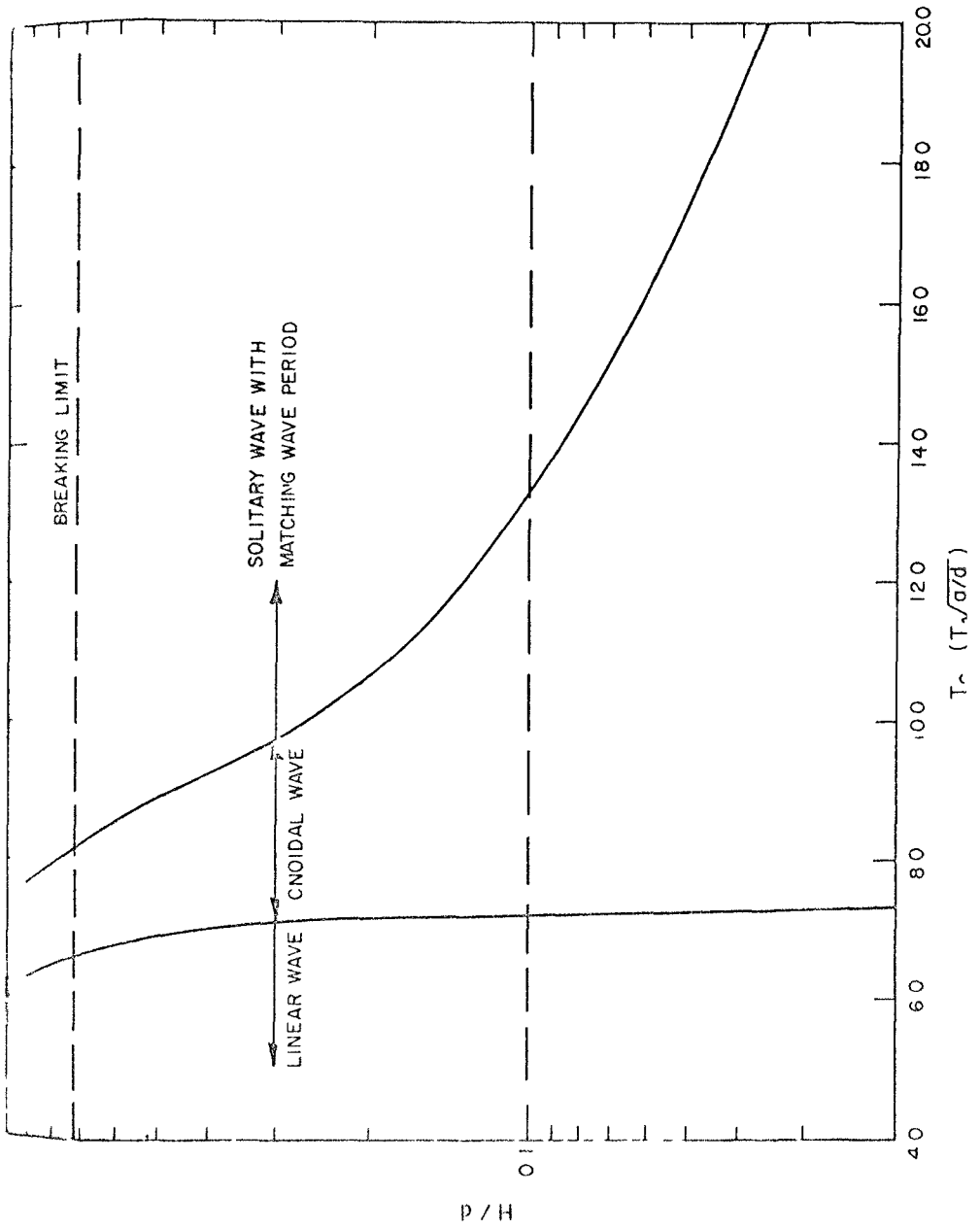


Figure 3 Region of wave theories

After several tests, the incremental interval $h = \Delta t/T$ was selected at $1/64$ throughout the computation

Input Conditions

The independent elements which affect the behavior of the body are

1 Environment

Wave height H
Wave period T
Water depth d
Gravity g

2 Fluid properties

Fluid density $\rho = 2.0$
Viscosity μ (Not explicitly involved, appears in terms of drag coefficients)

3 Submerged body

Length ℓ
Cross sectional areas along the longitudinal coordinate S_1
($i = 1$ to m number of station)
Longitudinal moment of inertia I_θ
Transverse moment of inertia I
Weight W
Metacentric height ee
Righting moment M_0
Added mass coefficients C_m 's

4 Initial conditions

Depth of submergence d_s
Velocity V_1
Angle of attack α_1
Form of first effective wave F
Orientating submerged body O

All of these factors are required inputs in the computer program

Numerical results

Figures 4 and 5 show, respectively, the vertical and horizontal displacements of the center of the body in a wave environment. In these figures, the free surface variation is drawn with respect to the gravity center of the submerged body. In the case of Figure 4, the body was initially placed at the middle water depth. The body has a tendency to surface. In the case of Figure 5, the body was placed right beneath the free surface, rose partially above the surface, and then dived down to hit the bottom, partially due to the additional downward force imposed on the body from the reduction of buoyancy force resulting from the surfacing.

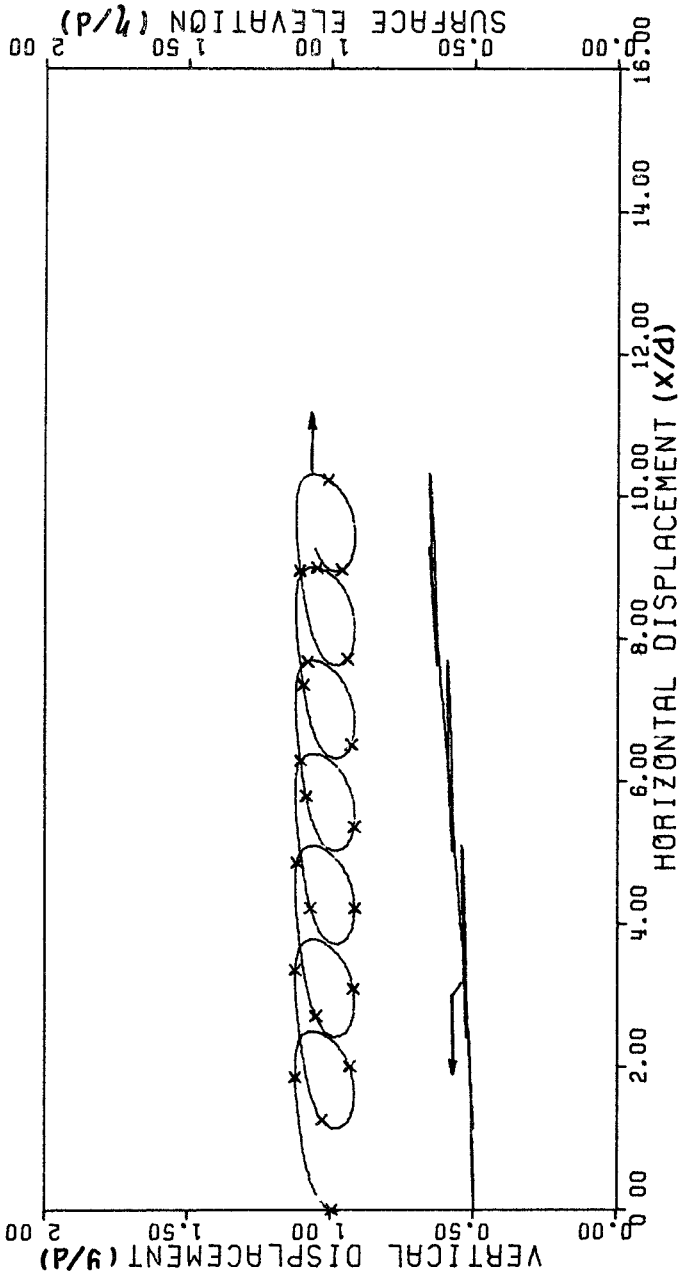


Figure 4 The locus of a submerged body which is initially placed at the middle depth

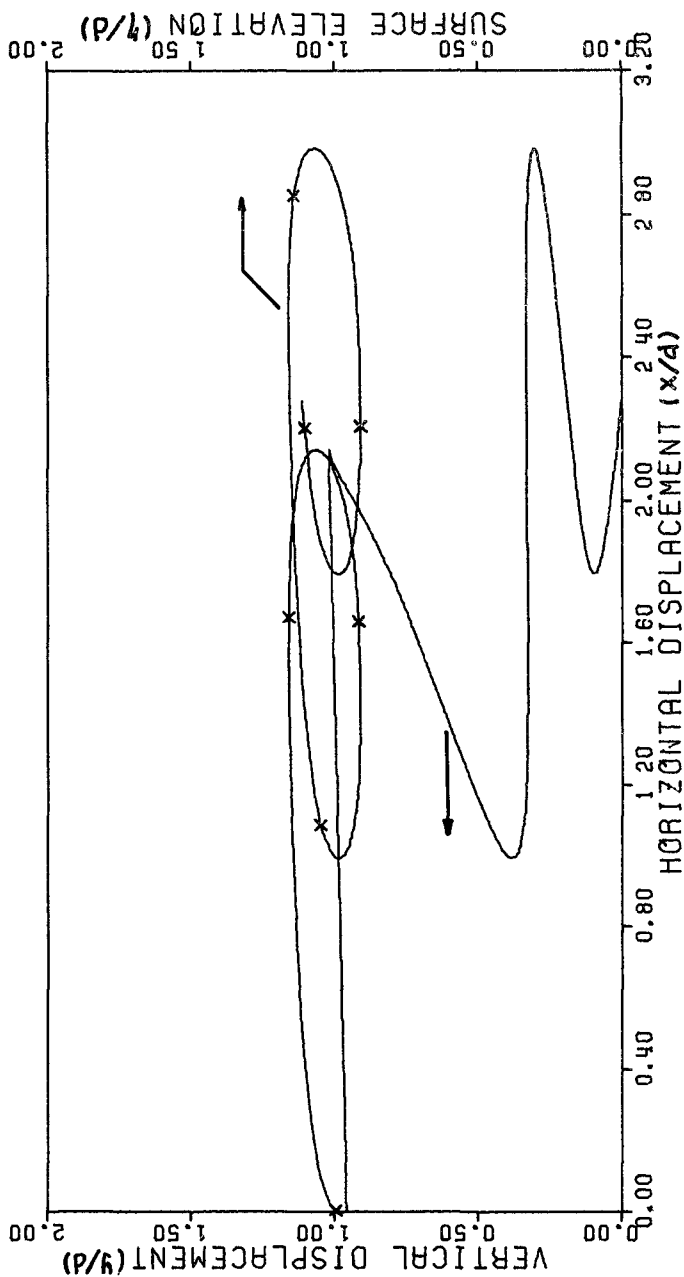


Figure 5 The locus of a submerged body which is initially placed right beneath surface

Figures 6 and 7 show the differences of the acceleration pattern of the body for different initial positions. The oscillation was more regular when the body was initially placed at mid-depth. The amplitude of the oscillation grew with time as the depth of the submergence decreased, as shown in Figure 4. Figure 7 shows the acceleration pattern for the case where the body was placed right beneath the free surface. The sudden increase of acceleration results from surfacing. Similar patterns were found for the heaving forces, which are closely related to these accelerations. A typical pitching motion is shown in Figure 8.

Discussion

The present work is to provide an analytical tool to examine the dynamic behavior of a submerged body when it is exposed in a shallow-water wave environment. A thorough investigation, considering every variable as listed in the previous section, though desirable, would be very cumbersome. Therefore, the consideration was restricted to specific hull configurations. Attempts were then made to examine the influence of environmental variables on the response of the structure. Even with such restriction, only qualitative evaluations can be made.

The wave height and the water depth were found to be the most influential variables. Dynamic stability, i.e., chance of capsize, depends significantly on them. Wave period is less important for the unsteady-state case considered. Original altitude of the body is also found to be of secondary importance, partially because the wave theories, even to the second order, yield hydrostatic pressure distribution in the vertical direction. This conclusion can not, however, be extended to the region where the body is close to the surface as illustrated in Figures 4 and 5.

The water inertia force, better known as the added mass effects, was found to vary with the altitude of the body. Correction was made by using experimentally determined added mass coefficients in the numerical computation. This coefficient, being approximately equal to 0.98 when the submergent depth is equal to or larger than six times the height of the body, decreases monotonically with the decreasing of submergence to a value of approximately 0.75 when the body is barely submerged. Further decrease in submergence will result in significant surface disturbance and was not considered. Because of the high waves used in the computation, it was found that the velocity-related force is no longer negligible. Entirely different results were obtained for the cases in which the velocity-related force was neglected, linearized and left to be proportional to the velocity square.

Also worth mentioning is the effect of the form of the first wave that encounters the body. Since waves are oscillatory in nature, the unsteady response of the body depends strongly on when the body is released in the wave cycle. In general, the body has a net translation in the wave direction when the first wave is in the form of a crest, whereas the net translation is opposite to the wave direction if the first wave is a trough. This phenomenon can easily be demonstrated experimentally.

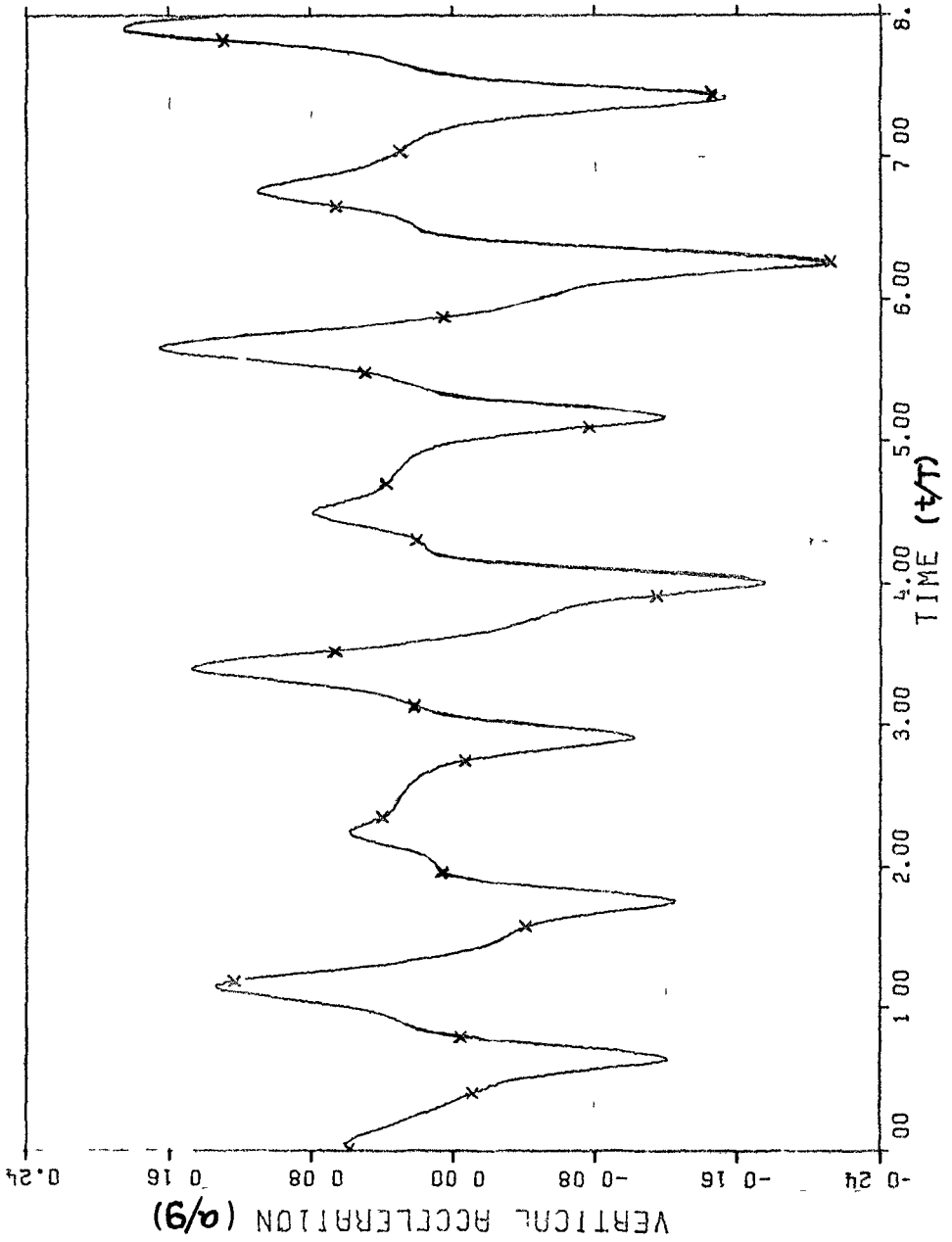


Figure 6 Vertical acceleration (mid-depth)

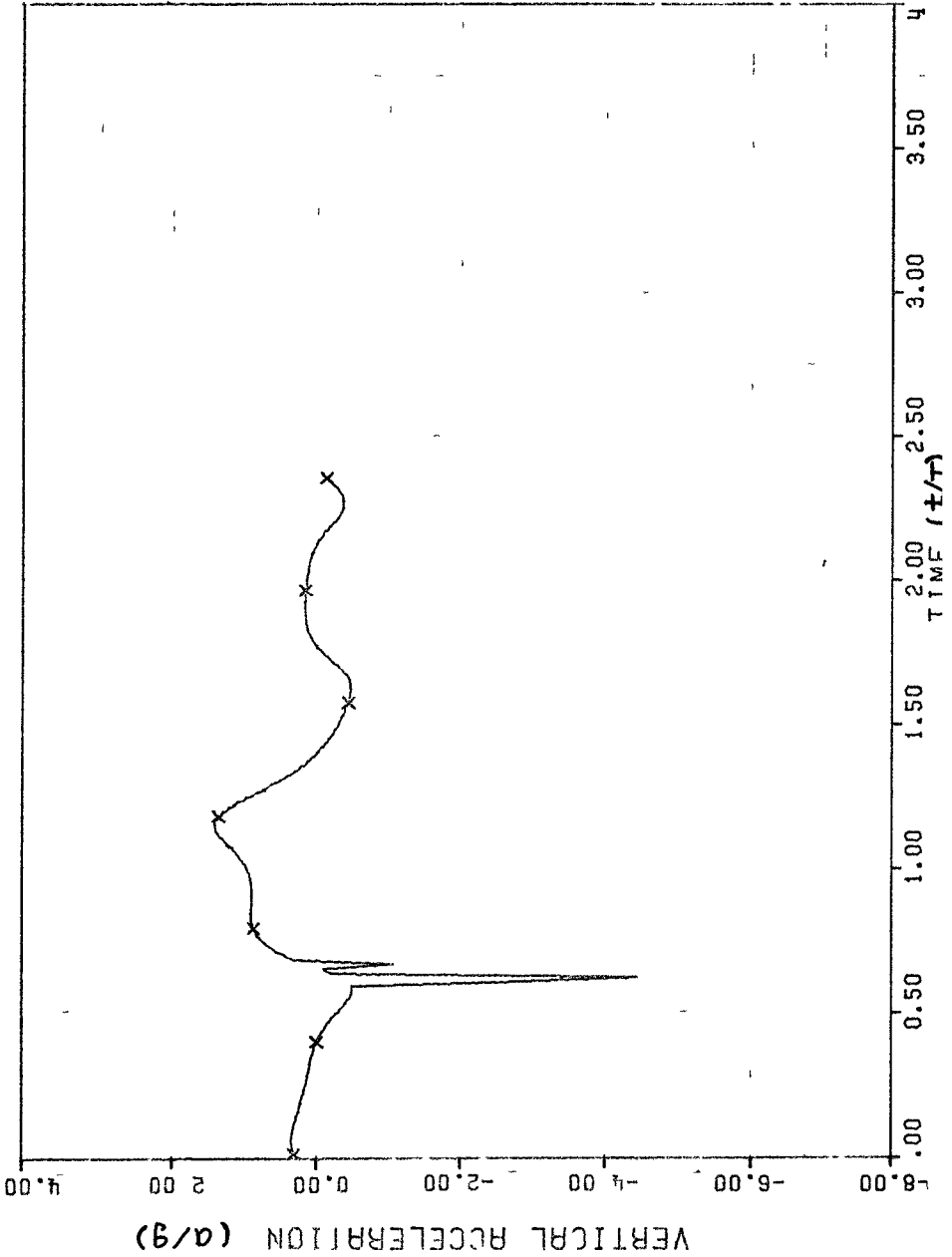


Figure 7 Vertical acceleration (beneath the free surface)

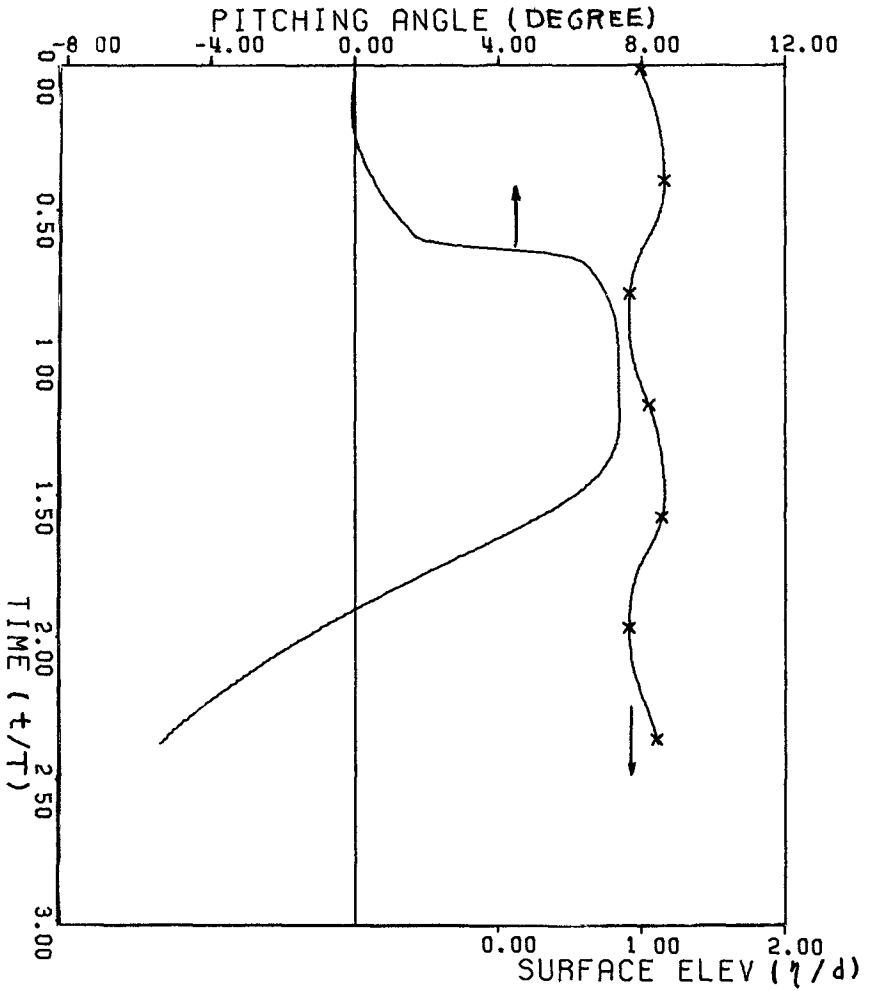


Figure 8 Pitching angle of a submerged body which is initially placed right beneath the free surface

Conclusion

Through analytical consideration, a numerical method was developed to suit the engineering purpose of quick assessment of the dynamic behavior of submerged slender body in high amplitude shallow water waves. To serve this purpose, as many variables as possible of engineering interest were included. In exchange, rigor in mathematics was compromised. Approximations such as strip theory, and empirical relations such as drag coefficient were used. Much desired are the future improvements of wave theory in shallow water region and a better understanding of velocity-related forces in oscillating fluid flows.

Acknowledgement

This work was performed under the sponsorship of ONR, and the authors would like to express their gratitude to Dr. B. LeMéhauté for his contribution.

References

- Hildebrand, F. B. (1956), Introduction to Numerical Analysis, McGraw-Hill Book Company, New York.
- Keulegan, C. H. and G. W. Patterson (1940), "Mathematical Theory of Irrotational Translation Waves," National Bureau of Standards Paper RP 1272.
- Korvin-Kroukovsky, B. V. (1961), Theory of Seakeeping, Society of Naval Architects and Marine Engineers, New York.
- Lamb, H. (1932), Hydrodynamics, 6th ed.